

Purdue Solar Cell Model (PSM) Version 2.0.0

Xingshu Sun, Raghu Vamsi Chavali, Sourabh Dongaonkar, Suhas Baddela, Mark
Lundstrom, and Muhammad Ashraful Alam

Purdue University
West Lafayette, IN 47907

Last Updated: April 10, 2017

1. Introduction	2
2. Verilog-A Implementation	2
-Definition of Terminal Voltage	2
-Intrinsic Current Components	3
-Parasitic Components	5
-Temperature-Dependence	5
-Numerical Smooth Function	5
3. Parameter Extraction	6
-Dark IV	6
-Illuminated IV	8
-Reverse breakdown IV	8
-Examples	9
4. Summary	11
Appendix	11
References	22

Introduction

Solar cells can be classified into three categories depending on the configuration: 1) P-N homojunction (Si, GaAs, etc.); 2) P-I-N junction (a-Si, Perovskites); 3) P-N heterojunction (CIGS, CdTe, HIT, etc.). The fundamental physics of carrier collection in each category of solar cells is distinct and shows different features in IV data. Hence, though compact models for solar cells may share some common circuit elements and physics, each one must be tailored to the specific technology being modeled.

At Purdue University, there is a large effort to develop a suite of physics-based compact models for various technologies, **Purdue Solar Cell Model (PSM)**, previously known as the TAG (technology agnostic) model (<https://nanohub.org/publications/20/1>). Specifically, solar cells of c-Si [1], a-Si [2], perovskites [3], CIGS [4], CdTe [5], and HIT [6] are modelled. Since the operation temperature of solar cells depends highly on the geographic location and local climates, the temperature dependence of the model is also properly accounted for. The development of the models is aimed at enabling photovoltaic system simulations to understand the roles of variability and reliability on the performance of solar modules as well as predict temporal energy yield for photovoltaics system in different environments and geographic locations, as discussed in [4]. A Matlab-based panel simulation builder will also be released along with the models. In this manual, we discuss the general features of the PSM model as well as the corresponding parameter extraction procedures. The compact model is described in **Verilog-A**, an industry standard modeling language for analog circuits.

2. Verilog-A Implementation

2.1 Definition of Terminal Voltage

As shown in Figure 1, the external terminals are labeled as vp (anode) and vn (cathode). The internal terminal labeled as vpi is separated from the external terminal by the resistor, R_{Series} , which represents the series resistance.

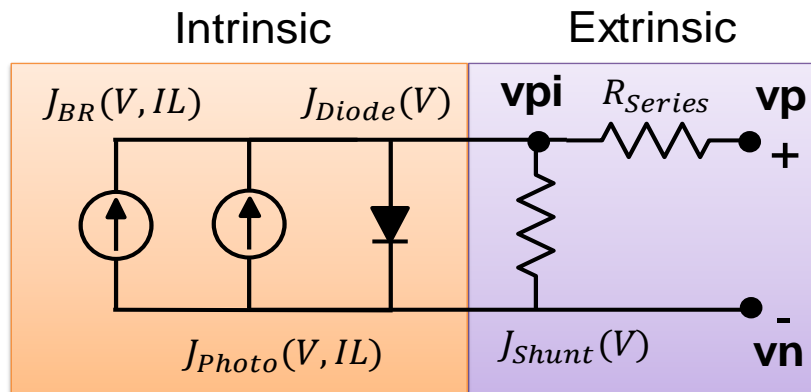


Fig. 1 Equivalent circuit incorporating the intrinsic components (orange box) and extrinsic components (purple box).

Voltage definitions:

$$\begin{aligned} V_i &= V(v_{pi}, v_n) \\ V_{re} &= V(v_p, v_{pi}) \end{aligned}$$

Branch definitions:

$$\begin{aligned} V_i &= V(v_{pi}, v_n) \\ V_{re} &= V(v_p, v_{pi}) \end{aligned}$$

For illustrative purpose, we will take the CIGS compact model to briefly introduce the analytical description of current components as well as its temperature dependency, see Sec. 2.2 to 2.5.

2.2 Intrinsic Current Components

It is common to model solar cells using the superposition principle: the current under illumination at a voltage, V , is the sum of the current in the dark at voltage, V , and the voltage-independent short circuit current under illumination. We write the light current as

$$J_{Light}(IL, V) = J_{SC}(IL) - J_{dark}(V). \quad (1)$$

where, $J_{dark}(V)$ is the dark current and $J_{SC}(IL)$ is the short circuit current. The photocurrent of c-Si cells is adequately described by the superposition principle. Thin-film solar cells are often more complicated. In general, we can describe their IV characteristics under illumination by a generalized superposition principle, namely,

$$J_{Light}(IL, V) = J_{Photo}(IL, V) - J_{Injection}(IL, V). \quad (2)$$

The diode injection current, $J_{Injection}(IL, V)$ or $J_{Diode}(IL, V)$, depends, in general, on both the applied voltage and on the optical generation, and may differ from $J_{dark}(V)$ due to the generation dependent recombination current. In general, the photocurrent, $J_{Light}(IL, V)$, depends on both the optical generation and on the applied voltage, therefore, may differ from $J_{Photo}(IL, V)$. To model thin-film solar cells, we must model these effects correctly.

2.2.1 Diode Current

One can analytically solve the drift and diffusion equations to obtain the diode current of a solar cell. Two considerations greatly simplify the equation for diode current for CIGS solar cells: 1) both numerical simulation and experimental data shows that the diode current in high-efficiency CIGS is illumination-independent; 2) measured data shows that the diode current can be expressed as

$$J_{Injection}(IL, V) \simeq J_{Diode}(V) = J_0(\exp(\frac{qV}{N \times kT}) - 1). \quad (3)$$

Here, J_0 is the reverse saturation current and the ideality factor, N , in (3) is a parameter between 1 and 2. Both of these two parameters are temperature dependent, as discussed in Sec. 2.4.

2.2.2 Photocurrent Current

By solving the drift-diffusion equations with the assumption of exponential generation profile and parabolic potential profile, an expression for bias-dependent photocurrent can also be derived. The result is

$$J_{Photo}(IL, V) \simeq J_{SC} \frac{1}{1 + \alpha_C \times \exp(\frac{q\beta(V_{Bi}-V)}{kT})}. \quad (4)$$

Here J_{SC} is the maximum photocurrent, α_C denotes the ratio between diffusion and thermionic emission velocities, V_{Bi} is the built-in potential across the junction, and finally, β is for voltage partition between the window/buffer layers and the absorber layer.

2.2.3 Breakdown Current

When one of the series-connected cells is shaded, the shaded cell will be stressed to reverse breakdown to maintain current continuity, hence heating up the module [7]. Hence, it is also very important to properly model reverse breakdown characteristics. We have developed a phenomenal model based on the Frenkel-Poole theory expressed as

$$J_{RB,D(L)}(IL, V) = J_{RB0,D(L)} \times V \times \exp(\frac{q}{kT} \sqrt{\frac{V}{m_{D(L)}}}), \quad (5)$$

where $J_{RB0,D(L)}$ is the pre-factor and $m_{D(L)}$ is the exponential index under dark (light) [5], [8]. The model has been validated against experimental data. This

breakdown current is included as a current source in the compact model, see Fig. 1.

2.3 Parasitic Components

2.3.1 Parasitic Shunt Current

The shunt current model consists of two parts. The first one describes the usual ohmic shunt conductance, and the second is Space-Charge-Limited (SCL) current transport, which has a non-ohmic characteristic. The semi-empirical formula used in the model is [3]

$$J_{Shunt} = G_{Shunt} \times V + I_{OShunt} \times V^\gamma. \quad (6)$$

The parameters, G_{Shunt} and I_{OShunt} , describe the ohmic and non-ohmic shunt components, respectively. The γ parameter is an exponent index with a typical range of 2 to 3, characteristic of SCL transport.

2.3.2 External Sheet Resistance

The second important parasitic component in solar cells is the external sheet resistance, which arises from the contact layer because the current must flow a certain distance before reaching the terminals. The finite resistance of the contact layers then causes extra output power loss. For simplicity, we use a single series-resistance parameter to describe the distributed sheet resistance. The sheet resistance is often higher at the module level, because it arises from the lateral current flow in metal/TCO layers. As a result, it should be noted that the value of r_{sheet} cannot be determined by fitting the IV characteristic of a single cell. The details of the physics are explained in Chapter 4 of [1].

2.4 Temperature-Dependence

Since the parameters of the model are physically defined, we can also analytically derive the temperature dependences of the parameter. For example, the T dependency of V_{Bi} of a heterojunction can be analytically described in terms of the bandgap, E_G , and the conduction band offset, ΔE_C [REF]. It has been experimentally shown that J_0 is linear with $e^{-E_G/N(T)kT}$ and $1/N(T) = 1/2 \times (1 + T/T^*)$ (assuming no tunneling) [9], where E_G is the absorber bandgap, and kT^* (ranging from 30 meV to 150 meV) is the characteristic slope of the exponentially distributed defects in the absorber. The complete list of the temperature-related equations is summarized in the appendix.

2.5 Numerical Smooth Function

In a module-level simulation, thousands of (individual) compact models represented by an equivalent circuit are connected in series and parallel, which can be numerically very expensive and challenging. In order to ensure convergence in the Newton-Raphson method, the model is designed to be numerical robust, i.e., the model function and its first-order and second-order derivatives are continuous, by implementing numerical smooth functions. For example, the discontinuous sign function in Verilog-A that returns the sign (1 and -1 for positive and negative, respectively) of the input (x) is replaced by a smooth function

$$\text{smoothsign}(x) = \tanh(k \times x), \quad (7)$$

where x is the input and k is the pre-factor [10]. All the numerical smooth function used in the model are listed in appendix.

*** Note: For all the models (CIGS/CdTe, HIT, Perovskite/a-Si, and c-Si), the exact equations and parameters implemented in Verilog-A files are summarized in the appendix.

3. Parameter Extraction

The purpose of Sec. 3 is to provide instructions to extract PSM model parameters from experimental or simulated data. This section is divided into two parts: dark IV and illuminated IV characteristics.

3.1 Dark IV:

A typical dark IV characteristic is shown in Figure 2. [4] Under low forward and reverse biases, the total current is dominated by the shunt current described by (7). The shunt current consists of two parallel components and can be described by (6). The parameters G_{shunt} , I_{0shunt} , and γ can be determined by fitting (7) to the reverse bias data. Please note that it is NOT recommended to fit the shunt current just using the low reverse bias current, such as from -0.2 V to -0.1 V. It will cause troubles later on due to the poor accuracy of the shunt conductance. The recommended voltage range to fit the shunt current is in the reverse bias from -1 V to 0 V in most cases. The fitting process can be achieved by the least square fitting function, “lsqcurvefit”, in Matlab or a tool named “PVanalyzer” [11] on PVhub (<http://nanohub.org/pvhub>).

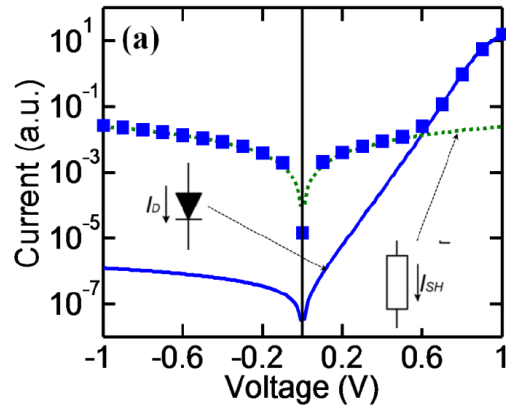


Fig. 2 (a) Typical dark IV of a solar cell (symbols) showing the diode (solid line) and shunt (dotted line) current components. (b) Conventional equivalent circuit representation of solar cells.

After obtaining the parameters for the shunt conductance, we can proceed to “clean” the dark IV to extract dark diode parameters. The voltage symmetry of the shunt current (i.e. $J_{shunt}(-V) = J_{shunt}(V)$) offers an easy method to separate the shunt and diode current components. Notice that the reverse current of the cell in Figure 2 is dominated by the shunt current. Thus, the forward diode current can be obtained simply by subtracting the reverse current from the forward current [4]. A comparison of original data and “cleaned” data is shown in Figure 3 [4].

By fitting the “cleaned” IV data to the diode equation with series resistance,

$$J_{Diode} = J_0 \left(\exp\left(\frac{q(V - J_{Diode} \times R_{Series})}{N \times kT}\right) - 1 \right). \quad (9)$$

we obtain the reverse saturation current, J_0 , the ideality factor, N , and the series resistance, R_{Series} . The series resistance, R_{Series} , obtained by this process is not the sheet resistance (r_{sheet}) in this model (the sheet resistance in the module level is usually higher than the series resistance of a single cell). Similarly to fit the shunt current, the fitting procedure can be done using either Matlab or “PVanalyzer” [11].

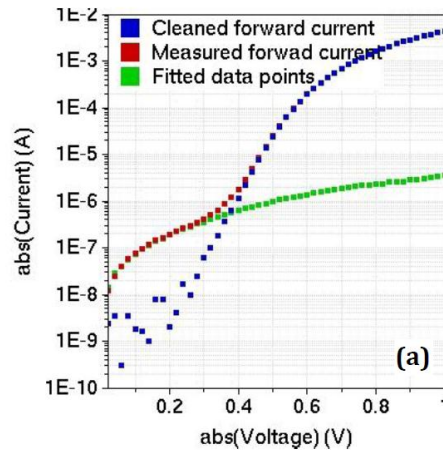


Fig. 3 Comparison of the measured current and the “cleaned” forward bias current.

3.2 Illuminated IV

The photocurrent, J_{photo} , is the difference between J_{Light} and J_{Dark} given that the diode current is illumination-independent. Therefore, one can extract $J_{Photo} = J_{Light} - J_{Dark}$ and fit it with the analytical equation for photocurrent using the Matlab fitting function, such as “lsqcurvefit”.

One can use the parameters obtained from here Sec. 3.1 as the initial guesses and tweak them to get the best fit of both light and dark IV curves. First, use the numbers obtained from the above steps as initial guesses then fit the dark IV using Matlab. Next, use the outputs from the previous step as initial guesses to fit light IV with the same technique. A couple of iterations should suffice to give a well-calibrated parameter set. We may need to sacrifice the fit of dark IV somewhat to fit the illuminated IV accurately, which is the priority.

3.3 Breakdown IV

For the avalanche breakdown model implemented in Si, HIT, Perovskite, and a-Si, one can use extrapolation to extract the parameter for breakdown voltage. The detailed procedures can be found in Sec. 3 of Ref. [12]

For the light-enhanced breakdown in CIGS/CdTe, it is recommended to subtract the shunt, diode current, photocurrent from the IV and then fit the pure breakdown IV with (5) using the Matlab fitting functions.

3.4 Example

All the models have been validated against sets of data [1], [3], [5], [6], [13], [14]. The benchmark results are summarized here. The data used in the benchmark are included in the model release packages, so are the corresponding parameters.

CIGS (Efficiency: ~18%):

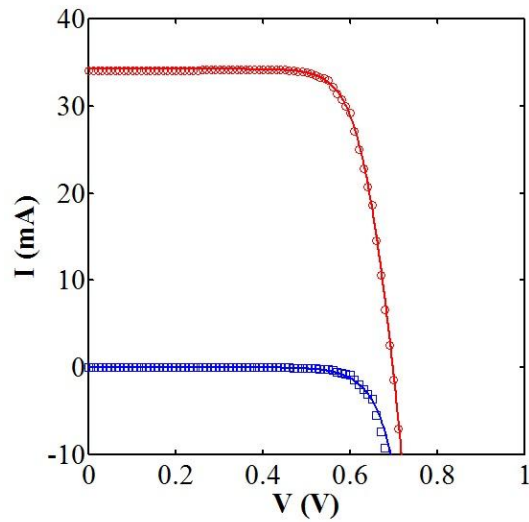


Fig. 4 The measured I-V (symbols) vs. the compact model (lines) at room temperature 294 K.

Perovskites (Efficiency: ~15.7%):

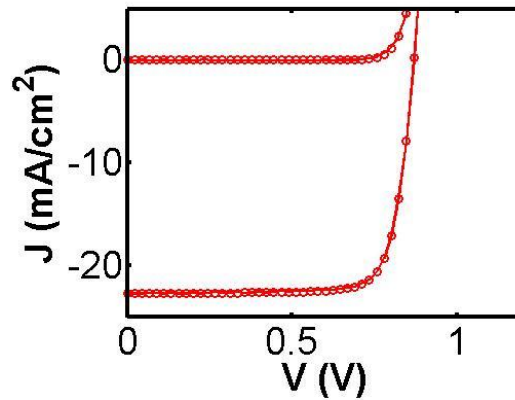


Fig. 5 The measured I-V (symbols) vs. the compact model (lines) at room temperature 300 K.

a-Si (Efficiency: ~3.3%):

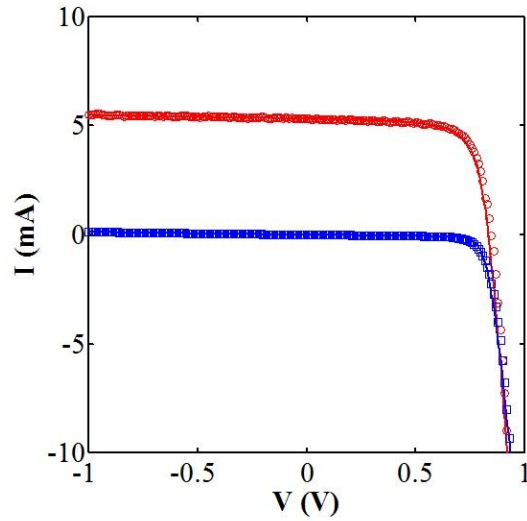


Fig. 6 The measured I-V (solid lines) vs. the compact model (symbols) at room temperature 300 K.

HIT (Efficiency: ~15.6 %):

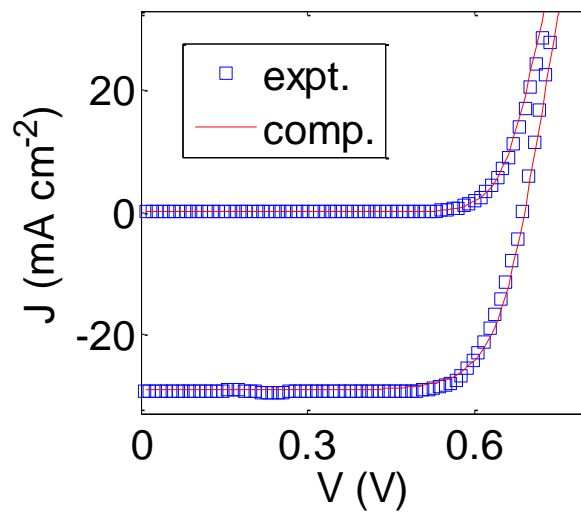


Fig. 7 The measured I-V (symbols) vs. the analytical model (line) at room temperature 300 K.

c-Si Module (110 W):

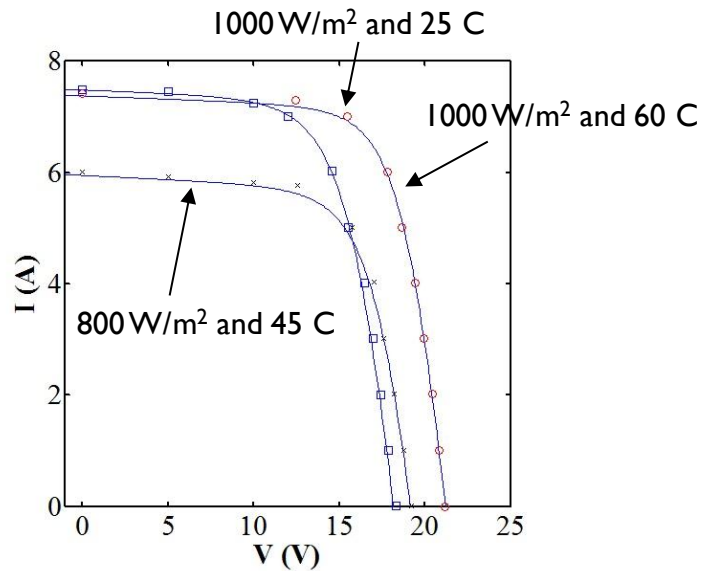


Fig. 8 Benchmark Results for PV module GEPV100.

4. Summary

The manual discusses the basic elements of the PSM solar cell model and the parameter extraction procedures. Future work involves improving the physics of the compact model (e.g., include time-dependent degradation model). Please contact sun106@purdue.edu regarding any questions/comments about the PSM solar cell model.

Appendix

Equation and Parameter List

All the equations and parameters used in the Verilog-A (va) files for all the PSM models (CIGS/CdTe, HIT, Perovskite/a-Si, and c-Si) are listed as below. The physical meanings of each of the parameters are also explained. The equation number is also referenced in the “va” files.

TABLE 1. The equations of the analytical model (CIGS/CdTe solar cells)

Analytical Equations for I-V Characteristics	
$j_{diode} = j0_{diode} * (\text{limexp}(V_i/kT/N) - 1)$	(T1.1)
$j_{shunt} = gsh1 * V_i + gsh2 * \text{pow}(V_i * \tanh(\text{smoothP1} * V_i), n_{sh})$	(T1.2)
$j_{photo} = fsmooth_f1 * (100 - \text{shading_P}) / 100 * jphoto_max / (1 + \text{betaV})$	(T1.3)
$j_{b1} = jb0_1 * V_i * \text{limexp}(mD/kT * \sqrt{V_i * \tanh(\text{smoothP1} * V_i)} + dV)$	(T1.4)
$j_{b2} = jb0_2 * V_i * \text{limexp}(mL/kT * \sqrt{V_i * \tanh(\text{smoothP1} * V_i)} + dV)$	(T1.5)
$j_b = (j_{b1} + fsmooth_f2 * j_{b2}) * fsmooth_f3$	(T1.6)
$I_{tot} = \text{area} * (j_{diode} - j_{photo} + j_{shunt} + j_b)$	(T1.7)
Illumination and Temperature Dependencies of Parameters	
$kT = T_{Cell} * 8.617e-5$	(T1.8)
$kTR = T_{REF} * 8.617e-5$	(T1.9)
$V_{bi} = EG + DEC + kT * ((V_{bi_REF} - (EG + DEC)) / kTR - \ln(\text{pow}(T_{Cell} / T_{REF}, 3)))$	(T1.10)
$\text{alphac} = \text{alphac_REF} * \text{limexp}(DEC/kT - DEC/kTR)$	(T1.11)
$N0 = 1.0 / N_{REF} - T_{REF} / T_{defect}$	(T1.12)
$N = 1.0 / (N0 + T_{Cell} / T_{defect})$	(T1.13)
$j0_{diode} = \text{limexp}(N_{REF} * \ln(j0_{diode_REF} / \text{limexp}(-EA/kTR/N_{REF})) / N) * \text{limexp}(-EA/kT/N)$	(T1.14)
$jb0_1 = jb0_1_REF * \text{limexp}(EITD/kTR - EITD/kT) * (\text{pow}(T_{Cell} / T_{REF}, 1.5))$	(T1.15)
$jb0_2 = jb0_2_REF * \text{limexp}(EITL/kTR - EITL/kT) * (\text{pow}(T_{Cell} / T_{REF}, 1.5))$	(T1.16)
Smooth Functions and Intermediate Variables	
$fsmooth_f1 = 0.5 * (1 - \tanh(\text{smoothP1} * (V_i - 0.99 * V_{bi})))$	(T1.17)
$fsmooth_f2 = -\tanh(0.02 * (\text{shading_P} - 100))$	(T1.18)
$fsmooth_f3 = 0.5 * (1 - \tanh(\text{smoothP1} * (1e-2 + V_i)))$	(T1.19)
$\text{betaV} = \text{alphac} * \text{limexp}(\text{beta} * (V_i - V_{bi}) / kT)$	(T1.20)

TABLE 2. The parameters of the analytical model (CIGS /CdTe solar cells)

General Parameters	
area	cell area [m ²]
shading_P	shading percentage [%]
T_REF	cell temperature for reference [K]
T_Cell	cell temperature [K]
Dark I-V Parameters	
j0_diode_REF	Reverse saturation current for reference [A/m ²]
N_REF	Diode ideality factor for reference
RS	Series resistance [Ω]
gsh1	Shunt conductance parameter 1 [S/m ²]
gsh2	Shunt conductance parameter 2 [S/m ²]
n_sh	Shunt conductance index
Light I-V Parameters	
jphoto_max	maximum photocurrent [A/m ²]
alphac_REF	ratio between $s_{n,f}$ and $s_{n,b}$ for reference
beta	voltage partition
Vbi_REF	cell built-in voltage for reference [V]
Breakdown I-V Parameters	
jb0_1_REF	FP pre-factor (dark) for reference [A/m ²]
jb0_2_REF	FP pre-factor (light) for reference [A/m ²]
mD	exponential index for dark breakdown current
mL	exponential index for light breakdown current
Parameters for Illumination and Temperature Dependencies	
EG	Energy bandgap of CIGS [eV]
EA	Activation Energy of j0 [eV]
DEC	Conduction band offset between CdS and CIGS [eV]
EITD	Defect level at dark [eV]
EITL	Defect level at light [eV]

T_defect	Defect characteristics temperature [K]
Parameters for Smooth Function and Numerical Stability	
smoothP1	smooth parameter for a continuous step function
dV	small number to make derivative continuous

TABLE 3. The equations for **perovskites and a-Si solar cells (p-i-n)**

Analytical equations for I-V characteristics	
$j_{\text{diode}} = (\text{alphaf} * j_{0f} + \text{alphab} * j_{0b}) * (\text{limexp}(V_i/kT) - 1)$	(T3.1)
$j_{\text{shunt}} = \text{gsh1} * V_i + \text{gsh2} * \tanh(\text{smoothP1} * V_i) * \text{pow}(\text{abs}(V_i), n_{\text{sh}})$	(T3.2)
$j_{\text{photo}} = (100 - \text{shading}_P) / 100 * j_{\text{photo_max}} * (-B * \text{limexp}(-m) + A)$	(T3.3)
$f_{\text{br}} = (1 - \text{limexp}(3 * (1 - \sqrt{((V_{\text{bi}} - V_{\text{br}}) / (V_{\text{bi}} - f_{\text{s1}} * f_{\text{s2}} * V_i))))))$	(T3.4)
$I_{\text{tot}} = \text{area} * (j_{\text{diode}} + j_{\text{photo}} + j_{\text{shunt}}) / f_{\text{br}}$	(T3.5)
Fitting parameters	
$VE = (V_i - V_{\text{bi}}) / kT$	(T3.6)
If (VE != 0)	(T3.7)
$\text{alphaf} = 1 / ((\text{limexp}(VE) - 1) / VE + \text{bf})$	(T3.7.1)
$\text{alphab} = 1 / ((\text{limexp}(VE) - 1) / VE + \text{bb})$	(T3.7.2)
Else	
$\text{alphaf} = 1 / (1 + \text{bf})$	(T3.7.3)
$\text{alphab} = 1 / (1 + \text{bb})$	(T3.7.4)
If (VE != m)	(T3.8)
$A = \text{alphaf} * ((1 - \text{limexp}(VE - m)) / (VE - m) - \text{bf})$	(T3.8.1)
Else	
$A = \text{alphaf} * (-1 - \text{bf})$	(T3.8.2)
If (VE != -m)	(T3.9)
$B = \text{alphab} * ((1 - \text{limexp}(VE + m)) / (VE + m) - \text{bb})$	(T3.9.1)
Else	
$B = \text{alphab} * (-1 - \text{bb})$	(T3.9.2)
Illumination and temperature dependencies of the parameters	
$kT = T_{\text{Cell}} * 8.617e-5$	(T3.10)
$V_{\text{br}} = V_{\text{br_REF}} * (1 + \beta_{V_{\text{br}}} * (T_{\text{Cell}} - T_{\text{REF}}))$	(T3.11)
Smooth Functions and Intermediate Variables	
$f_{\text{s1}} = 0.5 * (1 - \tanh(\text{smoothP1} * V_i))$	(T3.12)
$f_{\text{s2}} = 0.5 * (1 + \tanh(\text{smoothP2} * (V_i - V_{\text{br}})))$	(T3.13)

TABLE 4. The equations of the for **perovskites and a-Si solar cells (p-i-n)**

General Parameters	
area	total cell area [m ²]
m	Absorber Thickness over lambda
shading_P	shading percentage [%]
T_REF	cell temperature of standard test condition (STC) [K]
T_Cell	cell temperature [K]
Dark I-V Parameters	
j0f	Front recombination current [A/m ²]
j0b	Back recombination current [A/m ²]
bf	Beta for front interface
bb	Beta for back interface
gsh1	Shunt conductance parameter 1 [S/m ²]
gsh2	Shunt conductance parameter 2 [S/m ²]
n_sh	Shunt conductance index
RS	series resistance [Ω]
Light I-V Parameters	
jphoto_max	maximum photocurrent [A/m ²]
Breakdown I-V Parameters	
Vbr_REF	breakdown voltage for reference [V]
Vbi	Cell built-in voltage [V]
Parameters for Illumination and Temperature Dependencies	
beta_Vbr	temperature dependence of breakdown voltage [1/C]
Parameters for Smooth Function and Numerical Stability	
smoothP1	smooth parameter for a continuous step function
smoothP2	Smooth parameter [V]

TABLE 5. The equations of the analytical model (**HIT solar cells**)

Analytical equations for I-V characteristics	
$j_{diode} = (j_{0_h_diode} * (\text{limexp}(V_i/kT/N_REF) - 1) / (\text{inv_sd} + \text{inv_s0} * \text{limexp}((-V_{sat_drk} + (1 - \text{pot_fact_drk}) * V_i) / (kT)))) + (j_{0_e_diode} * (\text{limexp}(V_i/kT) - 1))$	(T5.1)
$j_{shunt} = g_{sh1} * V_i + g_{sh2} * \tanh(\text{smoothP1} * V_i) * \text{pow}(\text{abs}(V_i), n_{sh})$	(T5.2)
$j_{photo} = (100 - \text{shading_P}) / 100 * j_{photo_max} * (\text{inv_sb} + \text{inv_sd}) / (\text{inv_sb} + \text{inv_sd} + \text{inv_s0} * \text{limexp}((-V_{sat_pho} + (1.0 - \text{pot_fact_pho}) * V_i) / (kT)))$	(T5.3)
$f_{br} = (1 - \text{limexp}(3 * (1 - \text{sqrt}((V_{bi} - V_{br}) / (V_{bi} - f_{s1} * f_{s2} * V_i))))$	(T5.4)
$I_{tot} = \text{area} * (-j_{photo} + j_{diode} + j_{shunt}) / f_{br}$	(T5.5)
Illumination and temperature dependencies of the parameters	
$kT = T_{Cell} * 8.617e-5$	(T5.6)
$kTR = T_{REF} * 8.617e-5$	(T5.7)
$j_{0_h_diode} = j_{0_diode_h_REF} * \text{pow}(T_{Cell} / T_{REF}, 3) * \text{limexp}(-(EG/kT - EG/kTR))$	(T5.8)
$j_{0_e_diode} = j_{0_diode_e_REF} * \text{pow}(T_{Cell} / T_{REF}, 3) * \text{limexp}(-(EG/kT - EG/kTR))$	(T5.9)
$V_{br} = V_{br_REF} * (1 + \beta_{Vbr} * (T_{Cell} - T_{REF}))$	(T5.10)
Smooth Functions and Intermediate Variables	
$f_{s1} = 0.5 * (1 - \tanh(\text{smoothP2} * V_i))$	(T5.11)
$f_{s2} = 0.5 * (1 + \tanh(\text{smoothP2} * (V_i - V_{br})))$	(T5.12)

TABLE 6. The equations of the analytical model (**HIT solar cells**)

General Parameters	
area	cell area [m ²]
shading_P	shading percentage [%]
T_REF	cell temperature for reference [K]
T_Cell	cell temperature [K]
Dark I-V Parameters	
j0_diode_h_REF	Reverse saturation current for reference (holes) [A/m ²]
j0_diode_e_REF	Reverse saturation current for reference (electron) [A/m ²]
N_REF	Diode ideality factor for reference
inv_sb	reciprocal of surface recombination velocity at back contact
inv_sd	reciprocal of drift velocity
inv_s0	reciprocal of emission velocity
Vsat_drk	Saturation voltage (diode current) [V]
pot_fact_drk	Voltage partition under dark
RS	series resistance [Ω]
gsh1	Shunt conductance parameter 1 [S/m ²]
gsh2	Shunt conductance parameter 2 [S/m ²]
n_sh	Shunt conductance index
Light I-V Parameters	
jphoto_max	maximum photocurrent [A/m ²]
Vsat_pho	Saturation voltage (photocurrent) [V]
pot_fact_pho	Voltage partition under light
Breakdown I-V Parameters	
Vbr_REF	Breakdown voltage for reference [V]
Vbi	Junction built-in potential
Parameters for Illumination and Temperature Dependencies	
EG	Energy bandgap at room temperature [eV]
beta_Vbr	Temperature dependence of breakdown voltage [1/C]

Parameters for Smooth Function	
smoothP1	smooth parameter for a continuous step function
smoothP2	Smooth parameter

TABLE 7. The equations of the analytical model (**c-Si solar modules**)

Analytical equations for I-V characteristics	
$j_{diode} = j01 * (\text{limexp}(V_i/kT/NS) - 1) + j02 * (\text{limexp}(V_i/kT/2/NS) - 1)$	(T7.1)
$I_{shunt} = V_i/RSH$	(T7.2)
$j_{photo} = jphoto_REF * (100-shading_P)/100 * (1+beta_jphoto * (T_Cell - T_REF))$	(T7.3)
$f_{br} = (1 - \text{limexp}(3 * (1 - \text{sqrt}((V_{bi} - V_{br}) / (V_{bi} - fs1 * fs2 * V_i / NS))))$	(T7.4)
$I_{tot} = (area * (j_{diode} - j_{photo}) + I_{shunt}) / f_{br}$	(T7.5)
Illumination and temperature dependencies of the parameters	
$kT = T_Cell * 8.617e-5$	(T7.6)
$kTR = T_REF * 8.617e-5$	(T7.7)
$EG = EG_REF * (1 + beta_EG * (T_Cell - T_REF))$	(T7.8)
$j01 = j01_REF * \text{pow}(T_Cell/T_REF, 3) * \exp(-(EG/kT - EG_REF/kT_REF))$	(T7.9)
$j02 = j02_REF * \text{pow}(T_Cell/T_REF, 2.5) * \exp(-(EG/kT - EG_REF/kT_REF)/2)$	(T7.10)
$RSH = RSH_REF * (100-shading_P)/100$	(T7.11)
$V_{br} = V_{br_REF} * (1 + beta_V_{br} * (T_Cell - T_REF))$	(T7.12)
Smooth Functions and Intermediate Variables	
$fs1 = 0.5 * (1 - \text{tanh}(\text{smoothP} * V_i / NS))$	(T7.13)
$fs2 = 0.5 * (1 + \text{tanh}(\text{smoothP} * (V_i / NS - V_{br})))$	(T7.14)

TABLE 8. The equations of the analytical model (**c-Si solar modules**)

General Parameters	
area	total cell area [m ²]
shading_P	shading percentage [%]
T_REF	cell temperature of standard test condition (REF) [K]
T_Cell	cell temperature [K]
NS	number of cells in a module
Dark I-V Parameters	
j01_REF	reverse saturation current 1 for reference [A/m ²]
j02_REF	reverse saturation current 2 for reference [A/m ²]
RS	series resistance [Ω]
RSH_REF	shunt resistance [Ω]
Light I-V Parameters	
jphoto_REF	maximum photocurrent for reference [A/m ²]
beta_jphoto	temperature coefficient of photocurrent [1/C]
Breakdown I-V Parameters	
Vbr_REF	breakdown voltage for reference [V]
beta_Vbr	temperature dependence of breakdown voltage [1/C]
Vbi	junction built-in potential [V]
Parameters for Illumination and Temperature Dependencies	
EG_REF	bandgap for reference [eV]
beta_EG	temperature dependence of EG [1/C]
Parameters for Smooth Function	
smoothP	smooth parameter

References

- [1] M. Hejri, H. Mokhtari, M. R. Azizian, M. Ghandhari, and L. Soder, "On the Parameter Extraction of a Five-Parameter Double-Diode Model of Photovoltaic Cells and Modules," *IEEE J. Photovoltaics*, vol. 4, no. 3, pp. 915–923, May 2014.
- [2] S. Dongaonkar and M. A. Alam, "End to end modeling for variability and reliability analysis of thin film photovoltaics," in *IEEE International Reliability Physics Symposium Proceedings*, 2012.
- [3] X. Sun, R. Asadpour, W. Nie, A. D. Mohite, and M. A. Alam, "A Physics-Based Analytical Model for Perovskite Solar Cells," *IEEE J. Photovoltaics*, vol. 5, no. 5, pp. 1389–1394, Sep. 2015.
- [4] X. Sun, T. Silverman, R. Garris, C. Deline, and M. A. Alam, "An Illumination- and Temperature-Dependent Analytical Model for Copper Indium Gallium Diselenide (CIGS) Solar Cells," *IEEE J. Photovoltaics*, vol. 1, pp. 1–10, 2016.
- [5] X. Sun, J. Raguse, T. J. Silverman, C. Deline, and M. A. Alam, "A physics-based compact model for CIGS and CdTe solar cells: from voltage-dependent carrier collection to light-enhanced reverse breakdown," *2015 IEEE 42nd Photovolt. Spec. Conf.*
- [6] R. V. K. Chavali, E. C. Johlin, J. L. Gray, T. Buonassisi, and M. A. Alam, "A Framework for Process-to-Module Modeling of a-Si/c-Si (HIT) Heterojunction Solar Cells to Investigate the Cell-to-Module Efficiency Gap," *IEEE J. Photovoltaics*, vol. 6, no. 4, pp. 1–13, Jul. 2016.
- [7] S. Dongaonkar, C. Deline, and M. A. Alam, "Performance and reliability implications of two-dimensional shading in monolithic thin-film photovoltaic modules," *IEEE J. Photovoltaics*, vol. 3, no. 4, pp. 1367–1375, 2013.
- [8] T. J. Silverman, M. G. Deceglie, X. Sun, R. L. Garris, M. A. Alam, C. Deline, and S. Kurtz, "Module-scale thermal and electrical effects of partial illumination in monolithic thin-film photovoltaics," *2015 IEEE 42nd Photovolt. Spec. Conf.*
- [9] U. Rau, a. Jasenek, H. W. Schock, F. Engelhardt, and T. Meyer, "Electronic loss mechanisms in chalcopyrite based heterojunction solar cells," *Thin Solid Films*, vol. 361, pp. 298–302, 2000.
- [10] J. Roychowdhury, "Dealing with Common Numerical Issues in Compact Models (Part 1)." [Online]. Available: <https://nanohub.org/resources/21262>.
- [11] S. Dongaonkar and M. A. Alam, "PV Analyzer," 2014. [Online]. Available: <https://nanohub.org/resources/pvanalyzer>.
- [12] M. C. Alonso-García and J. M. Ruíz, "Analysis and modelling the reverse characteristic of photovoltaic cells," *Sol. Energy Mater. Sol. Cells*, vol. 90, no. 7–8, pp. 1105–1120, May 2006.
- [13] J. E. Moore, S. Dongaonkar, R. V. K. Chavali, M. A. Alam, and M. S. Lundstrom, "Correlation of built-in potential and I-V crossover in thin-film solar cells," *IEEE J. Photovoltaics*, vol. 4, no. 4, pp. 1138–1148, 2014.
- [14] R. V. K. Chavali, S. Khatavkar, C. V. Kannan, V. Kumar, P. R. Nair, J. L. Gray, and M. A. Alam, "Multiprobe Characterization of Inversion Charge for Self-Consistent Parameterization of HIT Cells," *IEEE J. Photovoltaics*, vol. 5, no. 3, pp. 725–735, May 2015.

